J Membrane Biol (2015) 248:865–881
DOI 10.1007/s00232-015-9825-6

Mathematical Models Describing Chinese Hamster Ovary Cell Death Due to Electroporation In Vitro

Janja Dermol[1] · **Damijan Miklavčič**[1]

Received: 21 January 2015 / Accepted: 16 July 2015 / Published online: 30 July 2015

Abstract Electroporation is a phenomenon used in the treatment of tumors by electrochemotherapy, non-thermal ablation with irreversible electroporation, and gene therapy. When treating patients, either predefined or variable electrode geometry is used. Optimal pulse parameters are predetermined for predefined electrode geometry, while they must be calculated for each specific case for variable electrode geometry. The position and number of electrodes are also determined for each patient. It is currently assumed that above a certain experimentally determined value of electric field, all cells are permeabilized/destroyed and under it they are unaffected. In this paper, mathematical models of survival in which the probability of cell death is continuously distributed from 0 to 100 % are proposed and evaluated. Experiments were performed on cell suspensions using electrical parameters similar to standard electrochemotherapy and irreversible electroporation parameters. The proportion of surviving cells was determined using clonogenic assay for assessing the ability of a cell to grow into a colony. Various mathematical models (first-order kinetics, Hülsheger, Peleg-Fermi, Weibull, logistic, adapted Gompertz, Geeraerd) were fitted to experimental data using a non-linear least-squares method. The fit was evaluated by calculating goodness of fit and by observing the trend of values of models' parameters. The most appropriate models of cell survival as a function of treatment time were the adapted Gompertz and the Geeraerd models and, as a function of the electric field, the logistic, adapted Gompertz and Peleg-Fermi models. The next steps to be performed are validation of the most appropriate models on tissues and determination of the models' predictive power.

Keywords Clonogenic assay · Cell death probability · Treatment planning · Electrochemotherapy · Predictive models · Non-thermal irreversible electroporation

Introduction

Electroporation is a phenomenon that occurs when short high voltage pulses are applied to cells and tissues. This exposure of cells to electric pulses results in pores being formed in the cell membrane. Membranes become permeable to molecules that cannot otherwise pass in or out of the cell (Kotnik et al. 2012; Weaver 1993). If the cell is able to recover, it is considered reversible electroporation. If the damage to the cell is too extensive and the cell dies, it is considered irreversible electroporation. The existence of the pores has been shown by molecular dynamics (Delemotte and Tarek 2012) and calculated by various theoretical models (Neu and Neu 2009; Weaver and Chizmadzhev 1996). Electroporation is already being used in medicine, e.g., electrochemotherapy (Edhemović et al. 2014), non-thermal irreversible electroporation as a method of tissue ablation (Cannon et al. 2013; Davalos et al. 2005; Garcia et al. 2014; Long et al. 2014; Neal et al. 2013), gene therapy (Daud et al. 2008; Heller and Heller 2010), DNA vaccination (Calvet et al. 2014), and transdermal drug delivery (Denet et al. 2004; Yarmush et al. 2014), as well as in biotechnology (Kotnik et al. 2015) and food processing (Mahnič-Kalamiza et al. 2014; Sack et al. 2010). It has been shown that a sufficient electric field (*E*-field) is the most important factor—all the cells in the tumor have to be permeabilized (in electrochemotherapy) (Miklavčič

✉ Damijan Miklavčič
damijan.miklavcic@fe.uni-lj.si

[1] Faculty of Electrical Engineering, University of Ljubljana, Tržaška 25, 1000 Ljubljana, Slovenia

et al. 1998) or irreversibly electroporated (in irreversible electroporation) to eradicate the tumor. *E*-field distribution also corresponds to tissue necrosis (Long et al. 2014; Miklavčič et al. 2000).

When performing electrochemotherapy, irreversible electroporation or gene therapy, fixed electrode configurations with predefined pulse parameters can be used (Heller et al. 2010; Mir et al. 2006). Alternatively, variable electrode configurations can be used when the target tumor is outside the standard parameters (Linnert et al. 2012; Miklavčič et al. 2012). When using variable electrode configurations, a plan is needed of the electrodes' position and the parameters of electric pulses that offer sufficient *E*-field in the tissue (Campana et al. 2013; Miklavčič et al. 2010; Neal et al. 2015; Šel et al. 2007; Županič et al. 2012). Treatment planning of electroporation-based medical applications has already been successfully used on colorectal liver metastases in humans (Edhemović et al. 2014), and on spontaneous malignant intracranial glioma in dogs (Garcia et al. 2011a, b). It is currently assumed in treatment plans that above an experimentally determined threshold value of *E*-field, all cells are permeabilized or destroyed and below this threshold cells are not affected or do not die—i.e., we assume a step-like response. In reality, though, the transition from non-electroporated to electroporated state and from reversibly to irreversibly electroporated state is continuous. Mathematical models of cell permeabilization and survival can be implemented in order to present treatment plan in a clearer way and to obtain a better prediction of the tissue damaged (Dermol and Miklavčič 2014; Garcia et al. 2014). In addition, mathematical models allow us to interpolate the predicted survival of the cells and predict survival for other parameters than those used for curve fitting. The mathematical models of survival have to be adaptable and describe the experimental data well (high goodness of fit). Goodness of fit is not only an important criterion but trends of the optimized values of the parameters and the predictive power of the model are also important. In an ideal case, the models would include all the parameters important for cell death due to electroporation, but would have the lowest possible number of parameters.

There are only a few reports describing the probability of cell permeabilization (Dermol and Miklavčič 2014) and cell survival after irreversible electroporation (Garcia et al. 2014; Golberg and Rubinsky 2010) using mathematical models. The first attempt using mathematical model of survival to describe cell death after irreversible electroporation was made by (Golberg and Rubinsky 2010). They successfully fitted the Peleg-Fermi model to experimental data of prostate cancer cells' death described in (Canatella et al. 2001). Later, (Garcia et al. 2014) simulated irreversible electroporation on liver tissue and characterized cell death using the Arrhenius rate equation for thermal injury and the Peleg-Fermi model for electrical injury. The authors determined that using commercially available bipolar electrodes (AngioDynamics, Queensbury, USA) and standard irreversible electroporation parameters (90 pulses, 100 μs duration, 1 Hz, 3000 V) most cell death is a consequence of electrical damage. In that study, the volume of the thermally destroyed tissue did not surpass 6 % of the whole destroyed volume and was concentrated in the immediate vicinity of the electrodes.

Until now, the Peleg-Fermi model has been the only mathematical model used for describing cell death as a consequence of irreversible electroporation in medicine. However, mathematical modeling of cell death has a long history in the field of microbiology, e.g., food sterilization (Peleg 2006). Most models from the field of microbiology describe thermal microbial inactivation; an independent variable is treatment time (t). We used these models (first-order kinetics, Weibull, logistic, adapted Gompertz, Geeraerd) in original and in transformed forms. In the original forms, the models remained unchanged, treatment time was an independent variable, and *E*-field was a parameter. In the transformed forms, *E*-field became the independent variable. There was no need to transform the Hülsheger model and the Peleg-Fermi model, since the independent variables were *E*-field and treatment time (Hülsheger et al. 1981) or *E*-field and the number of pulses (Peleg 1995). In existing studies, mathematical models have not yet been used as a function of the *E*-field. Since *E*-field is a dominant parameter for predicting the effect of the electroporation, we were interested in obtaining models as a function of *E*-field. We also provide an explanation of the reasoning for the transformation for each of the transformed models.

In (Canatella et al. 2001), the authors exposed prostate cancer cells to 1–10 exponentially decaying pulses in the range of 0.1–3.3 kV/cm, with time constants in the range of 50 μs–20 ms. In our experiments, up to 90 square pulses, 0–4.0 kV/cm, 50–200 μs were applied, which are typically used in electrochemotherapy and irreversible electroporation treatments. Clonogenic assay was used as a measure of the ability of the cells to reproduce (Franken et al. 2006).

Our study is the first attempt to compare different mathematical models describing the survival of animal cells due to electroporation. We present the results obtained with electrical parameters similar to those typically used in electrochemotherapy and in irreversible electroporation clinical treatments. We evaluate the trends/meaning of the parameters of the mathematical models, determine whether and which models could be used for describing cell death, and which models should be validated in the treatment planning and treatment response prognostics of electrochemotherapy and irreversible electroporation.

Materials and Methods

Cell Preparation and Electroporation

Chinese hamster ovary cells (CHO-K1; European Collection of Cell Cultures, Great Britain) were grown in 25-mm^2 culture flasks (TPP, Switzerland) for 2–3 days in an incubator (Kambič, Slovenia) at 37 °C and humidified 5 % CO_2 in HAM-F12 growth media (PAA, Austria) supplemented with 10 % fetal bovine serum (Sigma Aldrich, Germany), L-glutamine (StemCell, Canada) and antibiotics penicillin/streptomycin (PAA, Austria), and gentamycin (Sigma Aldrich, Germany). The cell suspension was prepared on the day of experiments. Cells were centrifuged and resuspended in potassium phosphate electroporation buffer (10 mM K_2HPO_4/KH_2PO_4 in a ratio 40.5:9.5, 1 mM $MgCl_2$, 250 mM sucrose, pH 7.4, 1.62 mS/cm, 260 mOsm) at a concentration 10^6 cells/ml.

A drop of cell suspension (100 µl) was pipetted between two parallel stainless steel electrodes (Fig. 1) with the distance between them set at 2 mm. The surface of the electrodes was much larger than the contact surface between the cell suspension and the electrodes. All the cells were thus exposed to approximately the same electric field, which was estimated as the voltage applied divided by the distance between the electrodes. Pulses were delivered using a Betatech electroporator (Electro cell B10 HVLV, Betatech, France) and monitored with an oscilloscope LeCroy WaveSurfer 422, 200 MHz and a current probe AP015 (both LeCroy, USA). The parameters of the applied electric pulses are summarized in Table 1. The electrodes were washed with sterile 0.9 % NaCl and dried with sterile gauze between samples. After pulse application, 80 µl of cell suspension was transferred into a microcentrifuge tube in which there was already 920 µl of HAM-F12. In the control, sample cells were put between the electrodes and no pulses were delivered. Control was performed at the beginning and at the end of each experiment to monitor whether the survival or number of cells in the suspension during an experiment had decreased. After all the samples had been exposed to electric pulses (10–20 min), cells were diluted in 0.9 % NaCl and plated in triplicates in 6-well plates (TPP, Switzerland) in 3 ml of HAM-F12. Different numbers of cells were plated, shown in Table 2 for parameters with different lengths of pulses and in Table 3 for parameters with different numbers of pulses (Franken et al. 2006). In preliminary experiments, we determined how many cells have to be seeded in order to obtain around 100 colonies per well. When more intense treatments (600 V, 50–90 pulses and 800 V, 30–90 pulses) were applied, often no cells survived but, because of experimental conditions, we could not seed more cells than the given number. Cells were grown for 6 days at 37 °C and 5 % CO_2.

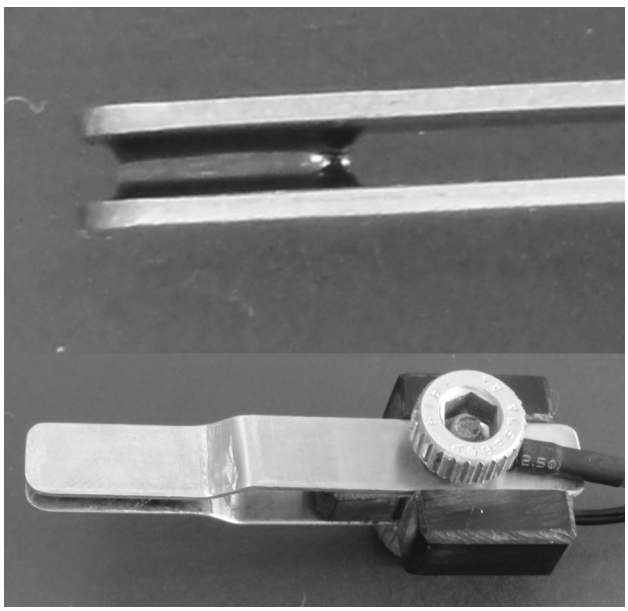

Fig. 1 Stainless steel parallel plate electrodes with a droplet of cell suspension between the electrodes (*upper image*). Inter-electrode distance is 2 mm

After 6 days, HAM-F12 was removed and cells were fixed with 1 ml of 70 % ethanol (Lekarna Ljubljana, Slovenia) per well. Cells were left in ethanol for at least 10 min, which rendered all cells dead. Colonies were colored with 200 µl of crystal violet (0.5 % w/v in distilled water) per well. Excessive crystal violet was washed away with pipe water. Colonies that had more than 50 cells were counted. The proportion of surviving cells (S) was calculated as

$$S = \frac{\text{number of colonies after the treatment}}{\text{number of seeded cells} \times \text{PE}}, \quad (1)$$

where plating efficiency (PE) is defined as

$$PE = \frac{\text{number of colonies formed in the control}}{\text{number of colonies seeded in the control}}. \quad (2)$$

The number of colonies formed in the control was calculated as an average of the triplicates of the colonies formed in the controls at the beginning and at the end of the experiment. The number of colonies seeded in control samples was 100. There was no difference between the two controls, so we could pool the results. At least four independent experiments were performed for each pulse parameter, and mean and standard deviation were then calculated.

In order to determine whether our pulses were indeed not causing significant heating, we measured the temperature of the cell suspension before any pulses were applied and within 5 s after the application of 90 pulses, 4.0 kV/cm, i.e., the most intense exposure. Because of the limitations of the temperature probe, the temperature could not be measured during the pulse application. We used the fiber optic sensor system ProSens (opSens, Canada) with a

Table 1 Experimental parameters of electric pulses, pulse repetition frequency 1 Hz

	Voltage/V	Electric field/kV/cm	Number of pulses/-	Pulse duration/μs
Varying pulse length	0–800, step 100	0–4, step 0.5	8	50, 100 or 200
Varying pulse number	0–800, step 200	0–4, step 1	30, 50, 70 or 90	100

Table 2 Number of plated cells in experiments with different lengths of the pulses, 8 pulses, 1 Hz pulse repetition frequency

Voltage/V	Electric field/kV/cm	Number of plated cells/-		
		For 50 μs	For 100 μs	For 200 μs
0	0	100	100	100
100	0.5	100	100	100
200	1.0	120	120	120
300	1.5	150	150	150
400	2.0	200	200	200
500	2.5	200	400	400
600	3.0	400	1000	1000
700	3.5	1000	2500	2500
800	4.0	2500	10,000	25,000

Table 3 Number of plated cells in experiments with different numbers of the pulses, 100 μs, 1 Hz pulse repetition frequency

Voltage/V	Electric field/kV/cm	Number of plated cells/-			
		For 30 pulses	For 50 pulses	For 70 pulses	For 90 pulses
0	0	100	100	100	100
200	1.0	120	150	200	200
400	2.0	1000	2500	25,000	25,000
600	3.0	25,000	25,000	25,000	25,000
800	4.0	25,000	25,000	25,000	25,000

fiber optic temperature sensor, which was inserted in the cell suspension between the electrodes. In addition, a numerical model of the cell suspension droplet between the electrodes was made and temperature distribution after 90 pulses of 4.0 kV/cm was calculated (Appendix).

Fitting of the Mathematical Models of Survival to the Experimental Results

Different mathematical models of survival were fitted to the experimental data: (i) the first-order kinetics model (Bigelow 1921), (ii) the Hülsheger model (Hülsheger et al. 1981), (iii) the Peleg-Fermi model (Peleg 1995), (iv) the Weibull model (van Boekel 2002), (v) the logistic model (Cole et al. 1993), (vi) the adapted Gompertz model (Linton, 1994), and (vii) the Geeraerd model (Geeraerd et al. 2000). The method of non-linear least squares was applied using Matlab R2011b (Mathworks, USA) and Curve fitting toolbox. Optimal values of the parameters of the mathematical models and R^2 values were determined. R^2 or the coefficient of determination is a statistical measure for the goodness of fit, i.e., it is a correlation between the predicted and experimentally determined values. Its values can be between 0 and 1 and the closer its value is to 1, the better the fit is. Natural logarithms of mathematical models were fitted to natural logarithms of the experimental data. This prevented the residuals at higher proportions of surviving cells from influencing the R^2 value the most. Treatment time t was understood as the time of exposure of cells to the electric field (E-field). It was calculated as

$$t = NT, \tag{3}$$

where N means number of the applied pulses and T the duration of one pulse.

The first-order kinetics model has a long history (Bigelow 1921):

$$S(t) = \exp(-kt). \tag{4}$$

Here, t denotes the time of exposure of bacteria to high temperature and k is the first-order parameter, i.e., the speed of decrease of the number of bacteria as a function of the duration of their exposure to heat.

Hülsheger studied the effect of E-field on *E. coli* and derived an exponential empirical model (Hülsheger et al. 1981):

$$S(t,E) = \left(\frac{t}{t_c}\right)^{\frac{-(E-E_c)}{k}}, \tag{5}$$

where k is a constant, which depends on the type of microorganism, E_c is the critical value of E-field below which there will be no inactivation (100 % survival), and t_c is the extrapolated critical value of t below which there will also be no inactivation.

The Peleg-Fermi model (Peleg 1995) has already been used for modeling irreversible electroporation (Garcia et al. 2014; Golberg and Rubinsky 2010) and is defined as

$$S(E,N) = \frac{1}{1+\exp\left(\frac{E-E_c(N)}{k(N)}\right)}, \tag{6}$$

$$E_c(N) = E_{c0}\exp(-k_1 N), \tag{7}$$

$$k(N) = k_0\exp(-k_2 N), \tag{8}$$

where E_c means critical E-field, N is the number of applied pulses, k is the kinetic constant that defines the slope of the curve, E_{c0} is the intersection of $E_c(N)$ with the y axis, k_0 is a constant in kV/cm, k_1 and k_2 are non-dimensional constants that depend on the parameters of the pulses and on the cells.

The Weibull model describes the time to failure of electronic devices after they have suffered some stress. The Weibull model is based on the observation that cells die at different times, which are statistically distributed. Cell death due to electroporation can also be described using the Weibull model (van Boekel 2002). We made a parallel: cell death as a function of E-field is also statistically distributed. In addition, no-one has so far observed any correlation between biological parameters and the parameters of the Weibull model. We thus transformed the Weibull model as a function of treatment time to a function of E-field. In previous studies, the independent variable was treatment time (time of exposure to high temperature or E-field). The Weibull model as a function of t is

$$S(t) = \exp\left(-\left(\frac{t}{b}\right)^n\right), \tag{9}$$

where t denotes time of exposure, b is a scale parameter, and n is a shape parameter. We can transform the Weibull model and obtain a model as a function of E:

$$S(E) = \exp\left(-\left(\frac{E}{b}\right)^n\right), \tag{10}$$

where all the parameters have the same meaning as in (9).

The logistic model can be used for describing distributions with a sharp peak and long tails (Cole et al. 1993). The logistic model is defined as

$$S(t) = 10^{\left(\frac{\omega-\alpha}{1+\exp\left(\frac{4\sigma(\tau-\log_{10}(t))}{\omega-\alpha}\right)}\right)}, \tag{11}$$

where parameter α denotes the common logarithm of the upper asymptote (survival around $t = 0$), ω the common logarithm of the lower asymptote (survival when $t \to \infty$), σ the maximum slope, and τ the position of the maximum slope. We measured the proportion of surviving cells. After a short treatment time, most of the cells are still alive, survival is 1. Therefore,

$$\alpha = \log(\text{upper asymptote}) = \log 1 = 0. \tag{12}$$

This allows us to simplify the Eq. (11) by assuming $\alpha = 0$:

$$S(t) = 10^{\left(\frac{\omega}{1+\exp\left(\frac{4\sigma(\tau-\log_{10}(t))}{\omega}\right)}\right)}, \tag{13}$$

where all the parameters have the same meaning as in (11).

A cumulative distribution of cell death was obtained in the experimental results. This means that the experimental data point of proportion of destroyed cells includes also cells that would already die at shorter treatment times or lower E-field values. A derivative of the cumulative cell death distribution shows how cell death is spread over different treatment times or E-field values; it shows cell death distribution. Because our experimental data was discontinuous, we obtained the derivative by calculating the difference in survival between two consecutive data points. We thus obtained the proportion of cells that die in a certain range of treatment time or E-field values, for example from 3000 to 5000 µs or from 1 to 2 kV/cm. Shorter treatment times or lower E-field values do not kill cells in that range. In dependence on the logarithm of the treatment time, the derivative of the cumulative cell death distribution (the derivative of experimental results) has a sharp peak and two long tails. A similar shape of cell death distribution is obtained as a function of E-field (without the logarithm). As already mentioned, the logistic model is suitable for distributions with a sharp peak and long tails. This was our basis for the transformation from treatment time as the independent variable to E-field as the independent variable. The model is

$$S(E) = 10^{\left(\frac{\omega}{1+\exp\left(\frac{4\sigma(\tau-E)}{\omega}\right)}\right)}, \tag{14}$$

where σ and τ have the same meaning as in (11) and ω denotes survival when $E \to \infty$.

The Gompertz model is usually used for describing growth of a tumor but in an adapted form it has also been used for cell survival (Linton 1994):

$$S(t) = \exp\left(Ae^{-e^{(B_0+B_1 t)}} - Ae^{-e^{B_0}}\right). \tag{15}$$

A denotes the natural logarithm of the lower asymptote, B_0 is the length of the upper asymptote, and B_1 is connected to the speed of cell death. B_1's absolute value determines the speed, the minus sign means a decrease in the number of

cells and plus means an increase. The adapted Gompertz model is purely empirical and was chosen because it offers an excellent goodness of fit. High R^2 is also obtained if the independent variable is E-field instead of treatment time. This was the reason for the transformation from treatment time as the independent variable to E-field as the independent variable. We transformed the adapted Gompertz model to a model as a function of E:

$$S(E) = \exp(Ae^{-e^{(B_0+B_1E)}} - Ae^{-e^{B_0}}), \quad (16)$$

where all the parameters mean the same as in (15).

Geeraerd defined a model that describes exponential decay of the number of surviving cells and a lower asymptote that models the remaining resistant cells (Geeraerd et al. 2000; Santillana Farakos et al. 2013):

$$S(t) = (Y_0 - N_{res})\exp(-kt) + N_{res}. \quad (17)$$

Y_0 means the number of cells at the beginning of experiments, N_{res} is the lower asymptote, and k is the specific inactivation rate (the slope of the exponentially decaying part of the curve). In our study, the number of cells was substituted by the proportion of cells in order to scale the model to our experimental data. At the beginning of our experiments, the proportion of survival was always 1. We simplified the Geeraerd model into

$$S(t) = (1 - N_{res})\exp(-kt) + N_{res}, \quad (18)$$

where all the parameters have the same meaning as in (17).

Results

Experimental Results

Figure 2 shows the experimental results—Fig. 2a for different pulse lengths and Fig. 2b for different numbers of pulses. Experimental results are shown in a semi-logarithmic scale, which enables low proportions of surviving cells to be visualized. It can be observed in Fig. 2a that longer pulses of the same electric field (E-field) cause lower survival. However, with 8, 200 µs pulses of 4.0 kV/cm, survival is still higher than with 50 or more 100 µs pulses of 4.0 kV/cm (Fig. 2b). When the E-field increases from 1.0 to 2.0 kV/cm, the survival after 50 pulses applied drops by two decades, while after 70 and 90 pulses it drops by three decades. In Fig. 2b, it can be seen that the experimental values of survival are very similar for 50, 70, and 90 pulses of 3.0 kV/cm and 4.0 kV/cm.

Results of the Mathematical Modeling

The results of the mathematical modeling are presented in two ways. First, Tables 4, 5, 6, and 7 summarize the optimal values of the parameters and R^2 values for all the mathematical models described in the Materials and Methods section. Figures 3, 4, 5, and 6 show plotted optimized mathematical models. When the results of the fitting are presented in linear scale, the curves go straight and exactly

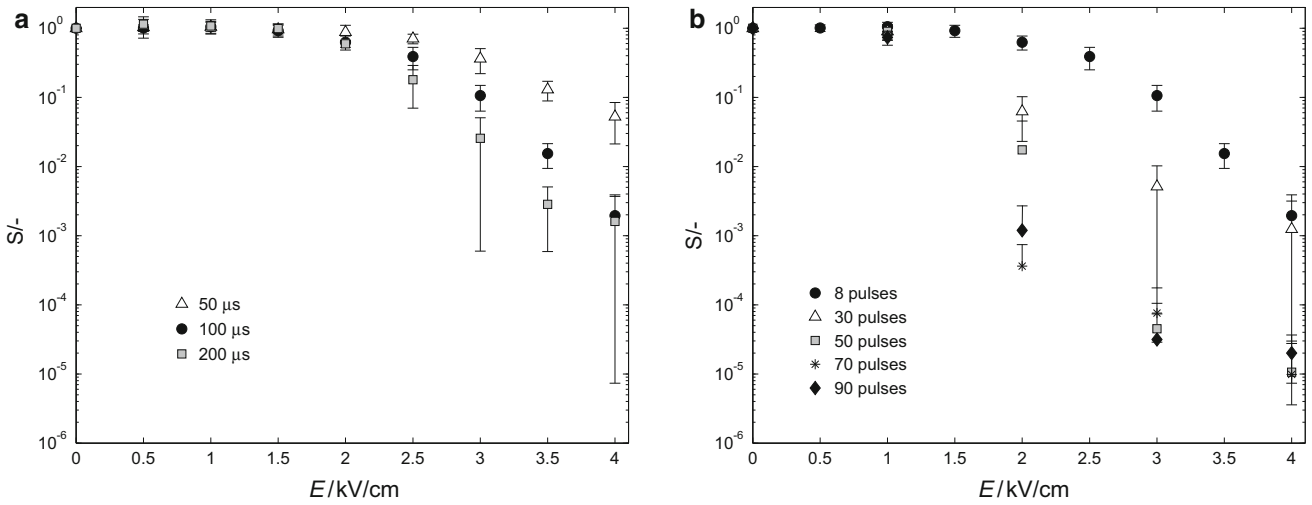

Fig. 2 Experimental results of the clonogenic assay for different pulse lengths (**a**) and for different numbers of pulses (**b**) as a function of the applied electric field (E). Mean ± one standard deviation is shown, pulse repetition frequency 1 Hz. If mean minus standard deviation is lower than 0, it cannot be presented in a semi-logarithmic scale and there is no error bar. The survival is lower when longer pulses are applied and the electric field is held fixed. However, higher number of pulses decreases the survival considerably. With 8, 200 µs pulses of 4 kV/cm, the survival is still higher than with 50 or more 100 µs pulses, 4 kV/cm

Table 4 Calculated optimal values of parameters of mathematical models as a function of treatment time and R^2 value for different electric field values

Mathematical models	Parameters	Optimized values of parameters and R^2 value		
		For 2.0 kV/cm (400 V)	For 3.0 kV/cm (600 V)	For 4.0 kV/cm (800 V)
First-order kinetics model (4)	k	0.0008805	0.001382	0.001582
	R^2	0.9096	0.8237	0.4747
Weibull model (9)	b	908	112	3.178
	n	0.8915	0.5490	0.3105
	R^2	0.9135	0.9442	0.9225
Logistic model (13)	ω	–3.925	–6.026	–20.760
	σ	–5.059	–4.240	–2.815
	τ	3.659	3.532	4.078
	R^2	0.9346	0.9607	0.9260
Adapted Gompertz model (15)	A	–8.18	–14.15	–16.05
	B_0	1.419	0.3732	1.8e-6
	B_1	–0.0004339	–0.0004419	–0.001291
	R^2	0.9389	0.9661	0.8539
Geeraerd model (18)	N_{res}	0.0005619	4.157e−5	4.014e−5
	k	0.001004	0.002011	0.007824
	R^2	0.9390	0.9788	0.8411

In all the experiments, pulses of 100 μs duration with pulse repetition frequency 1 Hz were applied

through the experimental results. In semi-logarithmic scale, deviations are more easily noticed. When fitting survival models to experimental results, it is advisable also to look at the data in semi-logarithmic scale. All our results are therefore presented in semi-logarithmic scale. When comparing the values of our optimized parameters with the values in other studies, it must be borne in mind that on the x axis there are t in μs or E-field in kV/cm.

Mathematical Models Describing Cell Survival as a Function of Treatment Time

A good fit could not be achieved using the Hülsheger model (5) because there were problems with the initial value of the parameters and local minima. The results are thus not shown and we do not discuss them.

In Fig. 3, (3.0 kV/cm, 100 μs, 1 Hz) it can be observed that the Weibull model (9), the logistic (13), the adapted Gompertz (15), and the Geeraerd models (18) are all similarly shaped and go very close to the experimental points. From the point of goodness of fit, they can be seen as equally good. The first-order kinetics model (4) is only able to describe a straight line in semi-logarithmic scale (Fig. 3, gray dashed line). It is unadaptable and offers low R^2 (0.47–0.90). Because of very low goodness of fit, the meaning of its parameters is not relevant.

Table 4 gives the optimized values of the parameters of the mathematical models as a function of treatment time. In the Weibull model (9), the values of n and b decrease with a higher applied E-field. In the logistic model (13), the value of the parameter ω decreases with higher E. The values of parameter τ are very similar. The values of σ increase with longer pulses, as expected (higher value, steeper slope). In the adapted Gompertz model (15), the values of parameter A decrease, which means a lower asymptote is reached. The values of parameters B_0 and B_1 also decrease, which means faster cell death with longer pulses applied. In the Geeraerd model (18), N_{res} corresponds to the remaining surviving cells and decreases with higher E (similar to parameter A in the Gompertz model). Parameter k corresponds to the speed of decrease and also increases, both as expected.

Mathematical Models Describing Cell Survival as a Function of Electric Field

In Fig. 4 (8, 100 μs pulses, 1 Hz), it can be observed that all models look very similar. The difference is in their behavior at high E-fields, i.e., in extrapolation of the data. In terms of goodness of fit, all four models on Fig. 4 (Peleg-Fermi (6), Weibull (10), logistic (14) and Gompertz (16)) can be considered equal.

In Fig. 5 (90, 100 μs pulses, 1 Hz), however, the differences among the models are more pronounced. They no longer overlap as shown in Fig. 4. The Peleg-Fermi (6) and Weibull models (10) go close but not exactly through the

Table 5 Calculated optimal values of parameters of mathematical models as a function of electric field and R^2 for different lengths of the pulses

Mathematical models	Parameters	Optimal values of parameters and R^2 value		
		For 50 μs	For 100 μs	For 200 μs
Peleg-Fermi model (6)	E_c/kV/cm	2.766	2.344	2.001
	k/kV/cm	0.4160	0.2677	0.2871
	R^2	0.9968	0.9975	0.9836
Weibull model (10)	b	2.992	2.408	1.936
	n	2.831	3.645	2.695
	R^2	0.9900	0.9964	0.9615
Logistic model (14)	ω	–1.555	–3.780	–2.961
	σ	–0.963	–1.888	–2.082
	τ	3.383	3.537	2.916
	R^2	0.9966	0.9951	0.9809
Adapted Gompertz model (16)	A	–5.348	–19.080	–7.692
	B_0	3.528	2.683	4.149
	B_1	–1.013	–0.6438	–1.505
	R^2	0.9987	0.9991	0.9961

In all the experiments, 8 pulses with pulse repetition frequency 1 Hz were applied

Table 6 Optimized values of parameters of mathematical models as a function of E and R^2 for different numbers of the pulses; the column 8 pulses is the same as the column 100 μs in Table 5

Mathematical models	Parameters and R^2	Optimal values of parameters and R^2 value				
		For 8 pulses	For 30 pulses	For 50 pulses	For 70 pulses	For 90 pulses
Peleg-Fermi model (6)	E_c (kV/cm)	2.3440	0.9720	0.9517	0.4298	0.4853
	k (kV/cm)	0.2677	0.4260	0.2446	0.2833	0.2852
	R^2	0.9975	0.8959	0.9637	0.9085	0.9148
Weibull model (10)	b	2.336	1.030	0.731	0.388	0.416
	n	3.410	1.439	1.480	1.076	1.098
	R^2	0.9989	0.9652	0.9408	0.9004	0.9039
Logistic model (14)	ω	–3.78	–2.93	–4.99	–4.58	–4.63
	σ	–1.888	–1.474	–3.308	–5.029	–4.483
	τ	3.537	2.260	2.243	1.754	1.863
	R^2	0.9951	0.9918	0.9989	0.9825	0.9995
Adapted Gompertz model (16)	A	–19.08	–7.23	–11.74	–10.82	–10.96
	B_0	2.683	2.439	3.849	3.372	3.348
	B_1	–0.643	–1.221	–1.894	–2.221	–2.037
	R^2	0.9991	0.9987	0.9999	0.9865	0.9999

In all the experiments, pulses of 100 μs duration with pulse repetition frequency 1 Hz were applied

experimental points (R^2 between 0.90 and 0.91), since they cannot model the lower asymptote but only a shoulder and then a constant decrease of cell survival (on a semi-logarithmic scale). The logistic and the adapted Gompertz models, on the other hand, go exactly through the experimental points ($R^2 > 0.99$) and also look very similar. From the point of view of the adaptability of the models, the logistic and Gompertz models are better than the Weibull (10) and Peleg-Fermi models (6).

Table 5 shows the results of fitting mathematical models as a function of E-field for different pulse lengths. The results of fitting the Peleg-Fermi model (6), the Weibull model (10), the logistic model (14), and the adapted Gompertz model (16) as a function of E-field are presented. For each model, the optimal values of the parameters and R^2 value for three different pulse durations (50, 100 and 200 μs) are shown.

Table 6 presents the results of fitting mathematical models as a function of E-field for different numbers of pulses. Optimal values of parameters and R^2 values for each fit are shown. The pulse length was held fixed at 100 μs. It can be seen that R^2 values are relatively high for

Table 7 Calculated optimal values of parameters of additional Peleg-Fermi mathematical models (7), (8) for E_c and k as functions of N

Mathematical models	Parameters	Optimal values of parameters and R^2 value
Peleg-Fermi mathematical model for $E_c(N)$ (7)	E_{co} (kV/cm)	2.734
	k_1	0.02506
	R^2	0.9237
Peleg-Fermi mathematical model for $k(N)$ (8)	k_0 (kV/cm)	0.3259
	k_2	0.001598
	R^2	0.04916

all the fits in Tables 5 and 6. The trends of the models are therefore analyzed more carefully for each of the models separately in the following paragraphs.

The plotted optimized Peleg-Fermi model (6) is presented in Fig. 6a. The Peleg-Fermi model (6) has an additional two models, which describe E_{c0} (7) and k (8) as functions of the number of pulses (N). Optimal parameters of these two models (7), (8) are plotted in Fig. 6b. In Fig. 6a, it can be seen that for higher numbers of pulses (50 or more), the model does not go exactly through the experimental points. For 8 and for 30 pulses, the Peleg-Fermi model describes the data very well, since there are no problems with modeling the lower asymptote. In Fig. 6b, it can be seen that Eq. (7) fits the experimental points well (black circles). However, Eq. (8) does not fit the data well (white squares on Fig. 6b), $R^2 = 0.049$. Equation (8) suggests an exponential dependence of k on the number of pulses, while in our data the value of k is almost constant.

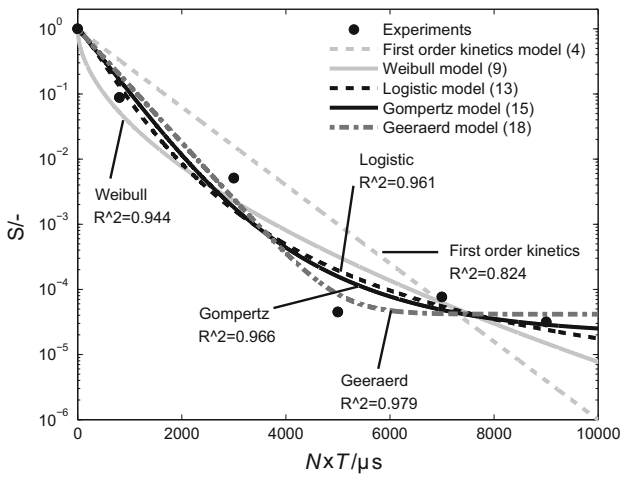

Fig. 3 Mathematical models (*lines*) and experimental results (*symbols*) showing cell survival as a function of the treatment time (3 kV/cm, 100 μs, 1 Hz). On y axis, there is the proportion of the surviving cells (S) in logarithmic scale. For each fit, R^2 value is shown. Except for the first-order kinetics model (4), all the models offer a good fit ($R^2 > 0.94$). We found the adapted Gompertz (15) and the Geeraerd model (18) to be the most suitable

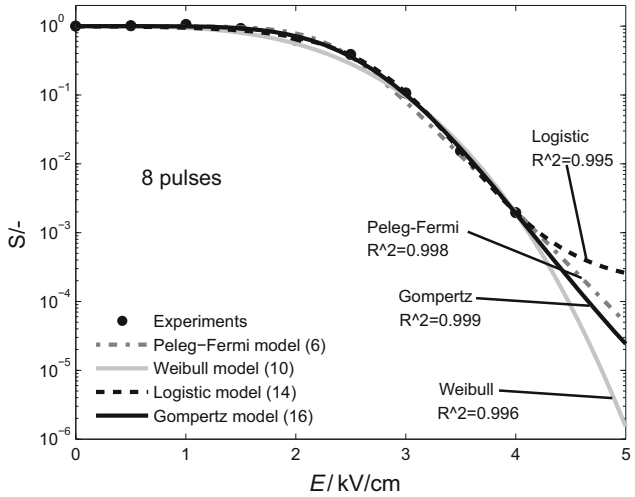

Fig. 4 Mathematical models (*lines*) and experimental results (*symbols*) showing cell survival as a function of electric field (8 pulses, 100 μs, 1 Hz). On y axis, there is the proportion of the surviving cells (S) in logarithmic scale. For each fit, R^2 value is shown. All the models as a function of electric field offer a similarly good fit ($R^2 > 0.99$). We found the adapted Gompertz (16), the Peleg-Fermi model (6)–(8), and maybe the logistic (14) model to be the most suitable

Table 7 presents additional results of fitting the Peleg-Fermi model, in which optimal values of the parameters and R^2 value for each fit of Eqs. (7) and (8) are shown. As already observed in Fig. 6b, Eq. (8) does not describe our data well. It can be observed that the goodness of fit is relatively high for the Peleg-Fermi model (>0.89) for different durations (Table 4), as well for different numbers of pulses (Table 5).

The Weibull model as a function of E-field (10) has a similar shape as the Peleg-Fermi model (6) (Fig. 5). The Weibull model cannot describe a sigmoid shape in semi-logarithmic scale, so a deviation at higher E-field of more than 8 pulses is noticeable (compare gray solid lines in Figs. 4 and 5). The meaning of the parameters of the Weibull model has not yet been established (10) and there is also no trend in the value of parameter n in our results. The value of parameter b decreases with longer pulses (Table 5) and with a higher number of pulses applied (Table 6).

The logistic (14) model is more adaptable and has a concave (Fig. 4) or sigmoid shape (Fig. 5) in semi-logarithmic scale. When fitting the logistic model (14) to the results of different pulse lengths (Table 5), σ decreases (faster death). Parameter τ denotes where on the x axis the decrease is fastest. It is similar for all pulse lengths (Table 5). When only 8 pulses of different lengths are applied (Table 5), the asymptote is not reached (Fig. 1a). Although the model predicts an asymptote, it is outside the

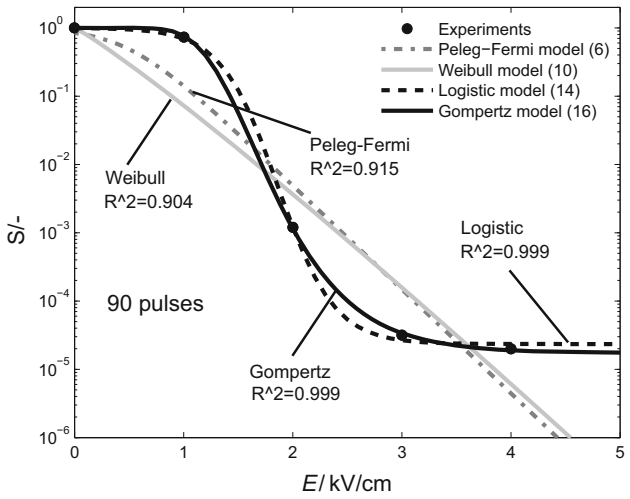

Fig. 5 Mathematical models (*lines*) and experimental results (*symbols*) showing cell survival as a function of electric field (90 pulses, 100 µs, 1 Hz). On *y* axis, there is the proportion of the surviving cells in logarithmic scale. For each fit, R^2 value is shown. Experimental values at 3 kV/cm and at 4 kV/cm (the lower asymptote) are on the limit of our detection. We found the adapted Gompertz (16), the Peleg-Fermi model (6)–(8), and maybe the logistic (14) model to be the most suitable

range in which our models are valid. In this case, the value of ω is not relevant since the models are not meant for extrapolation of the data. When fitting the logistic model to the results of different numbers of pulses, the parameters cannot be so easily explained. Parameter ω is similar with more pulses applied (Table 6) since we reach a similar lower asymptote (Fig. 1b). Parameter σ is similar for 70 and 90 pulses and on average higher than for 30 and 50 pulses. This means faster cell death when 70 or 90 pulses are applied. Parameter τ mostly decreases with a higher number of pulses applied (Table 6), which means that cells die at lower *E*-fields when more pulses are applied.

When applying the adapted Gompertz model (16) to the results of different pulse lengths, the values of parameter *A* are quite different (Table 5) because the lower asymptote was not reached in the experiments (Fig. 2a). Parameter *A* also does not have a trend with different numbers of pulses applied (Table 6), but the reason could be that with 50, 70, or 90 pulses, there is a similar proportion of surviving cells at higher *E*-field (around 10^{-5}). Parameters B_0 and B_1 in Table 5 have similar values since the experimental values for different lengths of the applied pulses are similar. The value of B_0 is similar for different numbers of pulses (Table 6) since it denotes the length of the upper asymptote, which is similar for all lengths of pulses (Fig. 5). B_1 decreases with more pulses (Table 6), which means faster death with more pulses applied.

Discussion

Several mathematical models are able to describe experimental results. The most appropriate models as a function of treatment time are the adapted Gompertz (15) and the Geeraerd models (18). The logistic model (13) can be used but a clearer meaning of its parameters needs to be established. The most appropriate models as a function of electric field (*E*-field) were the Peleg-Fermi (6), the logistic (14), and the adapted Gompertz models (16). Mathematical models of cell survival could thus be integrated into treatment planning of electrochemotherapy and irreversible

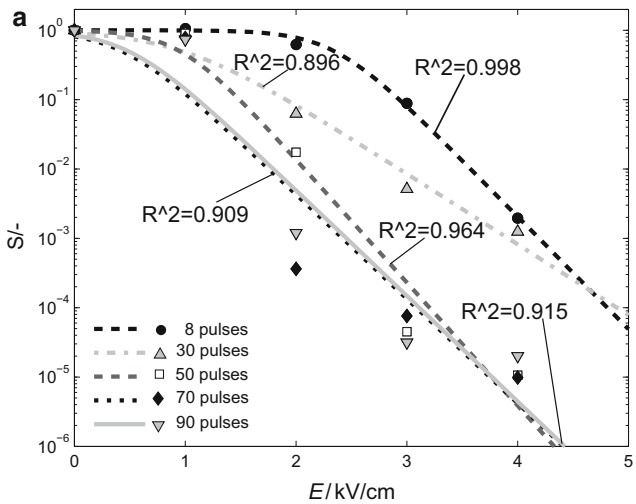

Fig. 6 The Peleg-Fermi model (6) for different numbers of pulses applied. For each fit, R^2 value is shown. **a** Symbols are the experimental values for 1 Hz, 100 µs, *lines* show the Peleg-Fermi model (6). **b** Symbols are the optimized values of E_c and *k*, *lines* show the optimized mathematical models (7) and (8). On *y* axis, there are the values of E_c and *k* in kV/cm. Since the Peleg-Fermi model (6) incorporates dependence on *E* as well as on *N* (7), (8) it already connects two treatment parameters (electric field and number of the pulses) and can therefore be used more easily than other models investigated in this study

electroporation as a method of tissue ablation. It must be emphasized that the models should not be extrapolated, since they predict different behaviors at very high *E*-fields or very long treatment time. Some of them keep on decreasing and some of them reach a stable value on a semi-logarithmic scale.

Experimental Considerations

The electrical parameters chosen for the experiments were similar to electrochemotherapy and irreversible electroporation electrical parameters typically used in vivo. For electrochemotherapy parameters, we used a fixed number of pulses (8) and we varied the length of the pulses. In electrochemotherapy treatments, 100 µs pulses are usually used but to evaluate the trend of the parameters of the mathematical models we also applied 50 µs and 200 µs pulses (results on Fig. 2a). For irreversible electroporation parameters, we tried to cover the parameter space as equally as possible. In an orthogonal space, where on one axis there was number of the pulses (*N*) and on the other *E*-field, we equidistantly sampled it by increasing the voltage by 200 V and the number of pulses by 30 (results on Fig. 2b).

An important aspect of irreversible electroporation experiments is the effect of increased temperature. Because of high voltage, many pulses, and high current, the temperature in the tissue or (as in our case) in the cell suspension can be increased considerably by Joule heating (Županič and Miklavčič 2011). Heating can change the conductivity of the cells, as well as damage them (Neal et al. 2012). Cell death could therefore be a thermal and not electrical effect (Garcia et al. 2014). The temperature of the suspension was therefore measured before and within 5 s after the end of application of 90 pulses, 4.0 kV/cm (the most severe electrical parameters employed in our study). Even with the most severe electrical parameters, the temperature within 5 s after the end of pulse application did not surpass 40 °C. This proved that, under our experimental conditions, cell death can indeed be considered solely as a consequence of irreversible electroporation.

The percentage of surviving cells was first evaluated using tetrazolium based assay (MTS assay). The MTS assay, however, proved not suitable for distinguishing between low proportions of surviving cells and it cannot be used to quantify the number of living cells exactly. The MTS assay is based on measurements of absorbance, which is then correlated to the number of metabolically active cells. After reaching 2 % of the surviving/metabolically active cells, the number did not drop, no matter how much higher an *E*-field or how many more pulses we applied. Since irreversible electroporation can be used successfully to treat tumors, a lower percentage of surviving cells should be achievable. In addition, metabolic activity and the ability to divide do not necessarily correlate. We therefore decided to use clonogenic assay, which requires more time than the MTS assay but enables exact quantification of the number of clonogenic cells. With more severe treatments, we could detect as low as 1 surviving cell in 25,000 (4×10^{-5} survival). In some experiments, the survival was lower than 4×10^{-5} because the final proportion of surviving cells was calculated as a mean over at least four repetitions. Often no cells survived (0 survival) with severe treatments. In calculating the mean, the 0 survival caused the final proportion of the survival to be lower than 4×10^{-5}. The detection limit of our clonogenic assay was thus reached at approximately 4×10^{-5}. The lower asymptote that can be observed in Fig. 2b for 50, 70, and 90 pulses at 3.0 and 4.0 kV/cm could be a consequence of the detection limit. For more precise (and lower), proportions of surviving cells at high *E*-field values and many pulses, more cells should be seeded, which can be achieved using a denser cell suspension. However, more precise results with denser cell suspension are perhaps not even needed. *In vivo*, the last few clonogenic cells seem to be eradicated by the immune system when performing electrochemotherapy (Calvet et al. 2014; Mir et al. 1992; Serša et al. 1997), as well as irreversible electroporation (Neal et al. 2013). The proportion of cells needed to kill to cause a complete response and destroy the whole tumor should be determined in future studies.

In our experimental results, we determined that the transition area between maximum and minimum survival gets narrower, i.e., the death of cells is quicker with higher numbers of pulses applied (Fig. 1b). This is in agreement with the theoretical predictions made (Garcia et al. 2014) using the Peleg-Fermi model. The authors predicted that the transition zone between electroporated and non-electroporated tissue becomes sharper when more pulses are applied.

There are also other parameters of the electric pulses, and biological parameters, which could affect the survival of cells. For example, the pulse repetition frequency in our experiments was always 1 Hz and when calculating the treatment time as $t = NxT$, we ignored the effect of pulse repetition frequency. There are contradicting studies that report on its effect on cell survival (Pakhomova et al. 2013; Pucihar et al. 2002; Silve et al. 2014). The effect of pulse repetition frequency on the shape of survival curves needs also to be investigated in future studies. It must be emphasized that even if $t_1 = t_2 = N_1T_1 = N_2T_2$ his cannot be necessarily understood as equal if $T_1 \neq T_2$ and $N_1 \neq N_2$. Different repetition frequencies affect cell permeabilization, and cell survival and temperature increase differently. We therefore present and discuss the results of different numbers and different lengths of applied pulses separately.

The value of *E*-field applied in the tissue is needed for correct prediction of surviving cells. At the moment, the most reliable method of determining *E*-field in tissues is numerical modeling. However, in future, the *E*-field in tissue could be monitored using current density imaging and magnetic resonance electrical impedance tomography (Kranjc et al. 2012, 2015). Cell survival in tissue could be correlated even better by taking into account conductivity changes (Kranjc et al. 2014) measured during application of the pulses.

One possible problem with prediction of cell death in tissues is the use of mathematical models fitted in vitro in an in vivo environment. Tissues, unlike cell suspensions, are heterogeneous; there are connections between cells; cells are irregularly shaped; extracellular fluid is more conductive than the pulsing buffer used in our study; and there is an immune system present. Before starting clinical studies, the parameters of electric pulses are first tested on cell lines. In the past, good correlation was found between the behavior of cells in vitro and in vivo. We expect survival curves in tissues to have a similar shape as in our in vitro study. The question is whether there will be a lower asymptote present or survival as a function of treatment time or *E*-field will keep decreasing. Our models can describe both options. The optimal values of the parameters depend on the sensitivity of the cells to the electric pulses and will probably be different. If the threshold values of the *E*-field for reversible and irreversible electroporation for different tissues are compared, different values can be found. For example, in vivo the threshold values of the *E*-field for muscle (8 × 100 µs pulses) for reversible electroporation have been determined to be 0.08 kV/cm and 0.2 kV/cm (parallel and perpendicular directions, respectively) and for irreversible electroporation to be 0.4 kV/cm (the same for parallel and perpendicular directions of muscle fibers) (Čorović et al. 2010, 2012). In vivo the threshold for irreversible electroporation of healthy prostate tissue has been determined to be 1 kV/cm (90 × 70 µs pulses) (Neal et al. 2014), and for healthy brain tissue 0.5 kV/cm (90 × 50 µs pulses) (Garcia et al. 2010). For healthy liver tissue, the threshold for reversible electroporation has been reported to be 0.36 kV/cm and for irreversible electroporation 0.64 kV/cm (Miklavčič et al. 2000). The thresholds thus seem to be different for different tissues (Jiang et al. 2015). *In vitro* the thresholds are usually higher and different for different cell lines: for reversible electroporation around 0.4 kV/cm and for irreversible electroporation around 1.0 kV/cm for 8 × 100 µs pulses (Čemažar et al. 1998). The curves in vivo can therefore be expected to have a similar shape but they will be scaled according to the thresholds for different types of tissue.

Mathematical Modeling

It was mentioned in the Introduction section that predictive power is one of the three most important criteria for choosing the model (in addition to goodness of fit and trends of values of the optimized parameters of the models). In our current study, however, predictive power was not assessed. For assessing predictive power, our optimized models must be validated on the samples for which the survival will be predicted. In our case, the models will be used in predicting death of tissues in electrochemotherapy and irreversible electroporation. Validation of the models on tissues is beyond the scope of this paper but must be done before implementing the models in actual treatment planning of electroporation-based treatments. The reader should also note that all the models approach 0 survival asymptotically but can never actually reach 0 survival. As already discussed, it is still not known how many cells must be killed to achieve a complete response of the tumor. Based on the fact that the immune system seems to eradicate the last remaining tumor cells, it seems that our models adequately describe 0 to 100 % survival. It remains to be established, however, what percentage of cells actually needs to be killed by irreversible electroporation.

Mathematical Models Describing Cell Survival as a Function of Treatment Time

We fitted the first-order kinetics (4), the Weibull (9), the logistic (13), the adapted Gompertz (15), and the Geeraerd (18) models to the experimental data as a function of treatment time. At 1.0 kV/cm (200 V), the percentage of surviving cells decreased to 68 % for 90 pulses, 100 µs, 1 Hz. The results of fitting the models to 200 V are thus not presented, since the decrease in survival was too small to be relevant for describing cell death due to electroporation.

It can be seen in Fig. 3 that, except for the first-order kinetics model (4), all the models describe the experimental points well. From the point of goodness of fit, the Weibull (9), the logistic (13), the adapted Gompertz (15), and the Geeraerd model (18) are equal. The next criterion is the trend of parameters which is to be discussed for each model separately in the next paragraph.

The first-order kinetics model (4) has a very low R^2 (Table 4) and it is not suitable for describing cell death. It is still very often used for describing microbial inactivation. (Peleg 2006) stated that the first-order kinetics model is popular because any data can be described with it if the data are sampled too sparsely. The second reason for its popularity is its long history. In the Weibull model (9), the parameters have a trend. However, in many studies, it has been shown that parameter n is not connected to any

biological or other parameter (Álvarez et al. 2003; Mafart et al. 2002; Stone et al. 2009; van Boekel 2002). It only describes the shape of the curve (concave, convex, linear). The Weibull model is often used because it is highly adaptable and can describe different shapes. Because the Weibull model was used in many previous studies, but the meaning of the parameters was not established in any of them, the Weibull model is most likely not suitable for predicting cell death after electroporation. The logistic model (14) has a high R^2 and most of its parameters can be connected to some biological parameter. It may be suitable for predicting cell death due to electroporation but the meaning of its parameters must be more clearly defined. In the adapted Gompertz model (16), both parameters B_0 and B_1 behave as expected (shorter upper asymptote and steeper decline). The Geeraerd model was defined for the shapes of curves just like ours—first the number of the cells exponentially decreases and, after a certain treatment time, it reaches a lower asymptote. The R^2 value was high and there was a trend of the values of the parameters.

It can be concluded that, as a function of treatment time, adapted Gompertz and Geeraerd models are suitable, while the logistic model has potential but should be tested with more electrical parameters.

Mathematical Models Describing Cell Survival as a Function of Electric Field

It can be seen in Fig. 4 that if there is no lower asymptote present, all the models describe the data well and have a similar R^2 value. In Fig. 5, a lower asymptote is present and the goodness of fit is different for different models. Looking at Figs. 4 and 5, it can be said that the logistic (14) and the adapted Gompertz models (16) are most suitable. In the Weibull model (10) (Tables 5, 6), there is no trend in the values of the optimized parameters. The Weibull model is not suitable for the use in treatment planning. The adapted Gompertz model (16) has high R^2 and the values of its parameters can be explained. The adapted Gompertz model is thus suitable for describing cell death after electroporation.

The logistic model (14) is highly adaptable. Because of the detection limit, not all values of the parameters behave as expected. Until the detection limit is reached (Fig. 2a), all the parameters can be explained (Table 5). It can therefore be said that the logistic model is probably suitable but it should be tested on a larger dataset.

We mentioned before that the Peleg-Fermi model (6) does not well describe cell death for higher numbers of the pulses. The reason is that it is not suitable for describing lower asymptotes. However, it is very likely that the lower asymptote is a consequence of the detection limit of the clonogenic assay. In this case, it is not problematic that the lower asymptote cannot be described. If it is discovered in vivo that there is a lower asymptote present, the usefulness of the Peleg-Fermi model will have to be evaluated separately for in vivo data. When the Peleg-Fermi model (6) was fitted to our in vitro experimental results, the E-field was the independent variable and the number of the pulses or their length was the parameters. Unfortunately, with different lengths of applied pulses, we could not model the change of $k(N)$ and $E_c(N)$, since there is no model to connect k and E_c with the length of the applied pulses. With different numbers of applied pulses (Table 6), we could also evaluate models for $E_c(N)$ (7) and $k(N)$ (8) (Table 7). The value of E_c decreases with a higher number of pulses (Table 6), is in agreement with our understanding of E_c as a critical E-field (Pucihar et al. 2011) and can be described using the proposed model (7). E_c changes less with a higher number of pulses. An even higher number of pulses applied would probably not lower the critical electric field but most likely only increase the heating. Values of k are approximately similar for all different numbers of applied pulses and they cannot be described using the proposed model (8). One reason may be the sensitivity of the clonogenic assay, as mentioned before. With more pulses, there could be even lower proportions of surviving cells, the model would be steeper and the value of parameter k would decrease. In (Golberg and Rubinsky 2010), the model was fitted to experimental data of up to 10 pulses applied, while in our study we fitted it to up to 90 pulses applied. Equation (8) may be exponential for up to 10 pulses applied but for more pulses it seems more like a constant. Equation (8) should be verified on tissues to see whether there is an exponential dependency. We assume that the Peleg-Fermi model (6), (7) will be suitable for use in treatment planning of electrochemotherapy and irreversible electroporation, while the dependency of parameter k on the number of pulses (8) remains questionable.

We next compared the values of our optimized parameters to the values reported in the literature. Our values of E_c and k are lower than in (Golberg and Rubinsky 2010) and optimized to describe the experimental results for 8–90 pulses. The authors in (Golberg and Rubinsky 2010) optimized their parameters to 1–10 pulses, whereby the decrease of the number of cells in dependency on the E-field is slower and smaller than for more pulses. This could explain the lower values of k and E_c as well as the non-exponential dependence of Eq. (8). The Peleg-Fermi model (6) seems the most promising of all the models analyzed in this study, since it also includes dependency on the number of pulses.

It can be concluded that the Peleg-Fermi (6), the adapted Gompertz (16), and probably also the logistic model (14) can all be used for describing cell death due to electroporation and could all be used in treatment planning of electrochemotherapy and irreversible electroporation.

Table 8 Parameters, used in our numerical model, with their symbols, values, and units

Name of the parameter	Symbol	Value	Units
Electrical conductivity	σ_s	0.162[S/m] × (1 + 0.02 × (T[degC]-20))	S/m
	σ_e	1.73913[MS/m] × (1 + 0.00094 × (T[degC]-20))	
Heat capacity at constant pressure	Cp_s	4200	J/(kg K)
	Cp_e	500	
Density	ρ_s	1000	kg/m^3
	ρ_e	8000	
Thermal conductivity	k_s	0.58	W/(m K)
	k_e	15	
Relative permittivity	ε_s	80	–
	ε_e	1	

Subscript *s* denotes cell suspension and subscript *e* denotes electrodes

Since the Peleg-Fermi model incorporates dependence on *E*-field as well as on the number of pulses it already connects two electrical parameters and can therefore be used more easily, while such connections still have to be determined for other models.

Conclusion

Mathematical models can describe cell death after electroporation. Hopefully, they can also be used in treatment planning of electrochemotherapy and irreversible electroporation as a method of tissue ablation. Mathematical models suitable for treatment planning have to describe the data well, have predictive power, and their parameters have to have a trend. Using the probability of cell death, the treatment plan can be made more reliable and also more comprehensive. Instead of displaying the electric field around the electrodes, the probability of tissue destruction around the electrodes can be shown. In this study, it was shown that not only the Peleg-Fermi but also other models are suitable for describing in vitro experimental results. However, it still needs to be determined whether the proposed mathematical models also have predictive and not just descriptive power. Our results are valid only for one cell line in suspension under our experimental conditions. The question is whether mathematical models could also be translated to tissues and more complex geometries. This validation should be done on tissues since the models will be used on tissues. Applying mathematical models of survival to tissues is thus the next step.

Acknowledgments This study was supported by the Slovenian Research Agency (ARRS) and conducted within the scope of the Electroporation in Biology and Medicine European Associated Laboratory (LEA-EBAM). Experimental work was performed in the infrastructure center 'Cellular Electrical Engineering' IP-0510. The authors would like to thank Dr. Bor Kos for his helpful comments about fitting of the models and numerical modeling and Lea Vukanović for her help with the experiments in the laboratory.

Appendix: Numerical Model of Temperature Distribution

We calculated temperature distribution to determine that 90, 100 μs pulses of 4 kV/cm and 1 Hz repetition frequency do not induce significant Joule heating. A numerical model of a drop of cell suspension between parallel plate electrodes was made in Comsol Multiphysics (v4.4, Comsol, Sweden) using Electric Currents, Heat Transfer, and Multiphysics modules in time-dependent analysis. Electrodes were modeled as two blocks of 20 × 10 × 1 mm and a drop of cell suspension was modeled as a block of 7 × 7 × 2 mm. Two boundaries, one on each electrode, were modeled as terminals, with +400 V and −400 V in the first 90 s of the simulation, while the other boundaries were electrically insulated. Similar as in (Garcia et al. 2011a, b), only one pulse was applied for 90 s, but we multiplied the Joule heating by the duty cycle (duration/period) to adjust the amount of delivered energy. We ran the simulation for an additional 5 s after the pulse application to validate the model with our temperature measurements, since measurements of temperature were made within 5 s after the pulse application.

The change of conductivity due to cell electroporation was disregarded in the model, since our cell suspension was dilute. The values of parameters used in the simulation are shown in Table 8. The properties of the cell suspension (except for electrical conductivity, which is characteristic of our electroporation buffer) are the same as for water.

The model was validated with current and temperature measurements at 90, 100 μs pulses, 4 kV/cm, 1 Hz repetition frequency. The predicted current (3.3 A) was in the same range as the measured current (from 2.9 to 3.5 A). Temperature measured within 5 s after the pulse application was 37.0 °C, while the predicted temperature 5 s after

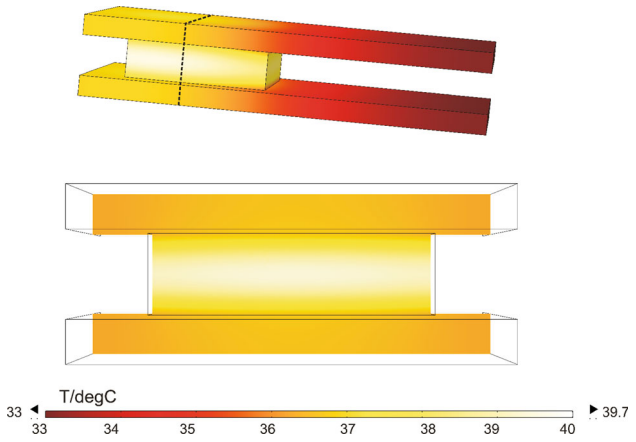

Fig. 7 Temperature distribution after 90, 100 µs pulses of 4 kV/cm. The *upper image* shows the temperature distribution on the surface of the electrodes and on the drop of the cell suspension. The *black dashed line* in the *upper image* shows where a cut plane for the lower image was made. The *lower image* shows a cut plane of the temperature distribution which goes through the middle of the electrodes. We can see that the temperature does not surpass 42 °C, therefore cell death can be ascribed solely to electroporation

the pulse application was 37.6 °C. The model thus adequately described our experiments.

The temperature distribution on the surface of the cell suspension and on the electrodes, and a slice through the drop of cell suspension after 90 pulses, is shown in Fig. 7. Since the temperature of the cell suspension does not exceed 42 °C, under our experimental conditions cell death can indeed be ascribed to electroporation.

References

Álvarez I, Virto R, Raso J, Condón S (2003) Comparing predicting models for the *Escherichia coli* inactivation by pulsed electric fields. Innov Food Sci Emerg Technol 4:195–202. doi:10.1016/S1466-8564(03)00004-3

Bigelow WD (1921) The logarithmic nature of thermal death time curves. J Infect Dis 29:528–536

Calvet CY, André FM, Mir LM (2014) Dual therapeutic benefit of electroporation-mediated DNA vaccination in vivo: enhanced gene transfer and adjuvant activity. OncoImmunology 3:e28540. doi:10.4161/onci.28540

Campana LG, Di Barba P, Dughiero F, Rossi CR, Sieni E (2013) Optimal needle positioning for electrochemotherapy: a constrained multiobjective strategy. IEEE Trans Magn 49:2141–2144. doi:10.1109/TMAG.2013.2241031

Canatella PJ, Karr JF, Petros JA, Prausnitz MR (2001) Quantitative study of electroporation-mediated molecular uptake and cell viability. Biophys J 80:755–764

Cannon R, Ellis S, Hayes D, Narayanan G, Martin RCG (2013) Safety and early efficacy of irreversible electroporation for hepatic tumors in proximity to vital structures. J Surg Oncol 107:544–549. doi:10.1002/jso.23280

Čemažar M, Jarm T, Miklavčič D, Maček Lebar A, Ihan A, Kopitar NA, Serša G (1998) Effect of electric-field intensity on electropermeabilization and electrosensitivity of various tumor-cell lines in vitro. Electro-Magnetobiology 17:263–272

Cole MB, Davies KW, Munro G, Holyoak CD, Kilsby DC (1993) A vitalistic model to describe the thermal inactivation of Listeria monocytogenes. J Ind Microbiol 12:232–239. doi:10.1007/BF01584195

Čorović S, Županič A, Kranjc S, Al Sakere B, Leroy-Willig A, Mir LM, Miklavčič D (2010) The influence of skeletal muscle anisotropy on electroporation: in vivo study and numerical modeling. Med Biol Eng Comput 48:637–648. doi:10.1007/s11517-010-0614-1

Čorović S, Mir LM, Miklavčič D (2012) In vivo muscle electroporation threshold determination: realistic numerical models and in vivo experiments. J Membr Biol 245:509–520. doi:10.1007/s00232-012-9432-8

Daud AI, DeConti RC, Andrews S, Urbas P, Riker AI, Sondak VK, Munster PN, Sullivan DM, Ugen KE, Messina JL, Heller R (2008) Phase I trial of interleukin-12 plasmid electroporation in patients with metastatic melanoma. J Clin Oncol 26:5896–5903

Davalos RV, Mir LM, Rubinsky B (2005) Tissue ablation with irreversible electroporation. Ann Biomed Eng 33:223–231. doi:10.1007/s10439-005-8981-8

Delemotte L, Tarek M (2012) Molecular dynamics simulations of lipid membrane electroporation. J Membr Biol 245:531–543. doi:10.1007/s00232-012-9434-6

Denet A-R, Vanbever R, Préat V (2004) Skin electroporation for transdermal and topical delivery. Adv Drug Deliv Rev 56:659–674. doi:10.1016/j.addr.2003.10.027

Dermol J, Miklavčič D (2014) Predicting electroporation of cells in an inhomogeneous electric field based on mathematical modeling and experimental CHO-cell permeabilization to propidium iodide determination. Bioelectrochemistry 100:52–61

Edhemović I, Brecelj E, Gasljevič G, Marolt Mušič M, Gorjup V, Mali B, Jarm T, Kos B, Pavliha D, Grčar Kuzmanov B, Čemažar M, Snoj M, Miklavčič D, Gadžijev EM, Serša G (2014) Intraoperative electrochemotherapy of colorectal liver metastases: electrochemotherapy of liver metastases. J Surg Oncol 110:320–327

Franken NAP, Rodermond HM, Stap J, Haveman J, van Bree C (2006) Clonogenic assay of cells in vitro. Nat Protoc 1:2315–2319

Garcia PA, Rossmeisl JH, Neal RE, Ellis TL, Olson JD, Henao-Guerrero N, Robertson J, Davalos RV (2010) Intracranial nonthermal irreversible electroporation. In vivo analysis. J Membr Biol 236:127–136. doi:10.1007/s00232-010-9284-z

Garcia PA, Pancotto T, Rossmeisl JH, Henao-Guerrero N, Gustafson NR, Daniel GB, Robertson JL, Ellis TL, Davalos RV (2011a) Non-thermal irreversible electroporation (N-TIRE) and adjuvant fractionated radiotherapeutic multimodal therapy for intracranial malignant glioma in a canine patient. Technol Cancer Res Treat 10:73–83

Garcia PA, Rossmeisl JH, Neal RE, Ellis TL, Davalos RV (2011b) A parametric study delineating irreversible electroporation from thermal damage based on a minimally invasive intracranial procedure. Biomed Eng OnLine 10:34

Garcia PA, Davalos RV, Miklavčič D (2014) A numerical investigation of the electric and thermal cell kill distributions in electroporation-based therapies in tissue. PLoS ONE 9:e103083

Geeraerd AH, Herremans CH, Van Impe JF (2000) Structural model requirements to describe microbial inactivation during a mild heat treatment. Int J Food Microbiol 59:185–209

Golberg A, Rubinsky B (2010) A statistical model for multidimensional irreversible electroporation cell death in tissue. Biomed Eng OnLine 9:13

Heller LC, Heller R (2010) Electroporation gene therapy preclinical and clinical trials for melanoma. Curr Gene Ther 10:312–317

Heller R, Cruz Y, Heller LC, Gilbert RA, Jaroszeski MJ (2010) Electrically mediated delivery of plasmid DNA to the skin, using

a multielectrode array. Hum Gene Ther 21:357–362. doi:10.1089/hum.2009.065

Hülsheger H, Potel J, Niemann EG (1981) Killing of bacteria with electric pulses of high field strength. Radiat Environ Biophys 20:53–65

Jiang C, Davalos RV, Bischof JC (2015) A review of basic to clinical studies of irreversible electroporation therap. IEEE Trans Biomed Eng 62:4–20. doi:10.1109/TBME.2014.2367543

Kotnik T, Kramar P, Pucihar G, Miklavčič D, Tarek M (2012) Cell membrane electroporation—Part 1: the phenomenon. IEEE Electr Insul Mag 28:14–23

Kotnik T, Frey W, Sack M, Haberl Meglič S, Peterka M, Miklavčič D (2015) Electroporation-based applications in biotechnology. Trends Biotechnol. doi:10.1016/j.tibtech.2015.06.002

Kranjc M, Bajd F, Serša I, Woo EJ, Miklavčič D (2012) Ex vivo and in silico feasibility study of monitoring electric field distribution in tissue during electroporation based treatments. PLoS ONE 7:e45737

Kranjc M, Bajd F, Serša I, Miklavčič D (2014) Magnetic resonance electrical impedance tomography for measuring electrical conductivity during electroporation. Physiol Meas 35:985–996

Kranjc M, Markelc B, Bajd F, Čemažar M, Serša I, Blagus T, Miklavčič D (2015) In situ monitoring of electric field distribution in mouse tumor during electroporation. Radiology 274:115–123. doi:10.1148/radiol.14140311

Linnert M, Iversen HK, Gehl J (2012) Multiple brain metastases—current management and perspectives for treatment with electrochemotherapy. Radiol Oncol. doi:10.2478/v10019-012-0042-y

Linton RH (1994) Use of the Gompertz Equation to Model Non-linear Survival Curves and Predict Temperature, pH, and Sodium Chloride Effects for Listeria monocytogenes Scott A. Faculty of the Virginia Polytechnic Institute and State University, Blacksburg

Long G, Bakos G, Shires PK, Gritter L, Crissman JW, Harris JL, Clymer JW (2014) Histological and finite element analysis of cell death due to irreversible electroporation. Technol Cancer Res Treat 13:561–569

Mafart P, Couvert O, Gaillard S, Leguerinel I (2002) On calculating sterility in thermal preservation methods: application of the Weibull frequency distribution mode. Int J Food Microbiol 72:107–113

Mahnič-Kalamiza S, Vorobiev E, Miklavčič D (2014) Electroporation in food processing and biorefinery. J Membr Biol 247:1279–1304

Miklavčič D, Beravs K, Šemrov D, Čemažar M, Demšar F, Serša G (1998) The importance of electric field distribution for effective in vivo electroporation of tissues. Biophys J 74:2152–2158

Miklavčič D, Šemrov D, Mekid H, Mir LM (2000) A validated model of in vivo electric field distribution in tissues for electrochemotherapy and for DNA electrotransfer for gene therapy. Biochim Biophys Acta BBA-Gen Subj 1523:73–83. doi:10.1016/S0304-4165(00)00101-X

Miklavčič D, Snoj M, Županič A, Kos B, Čemažar M, Kropivnik M, Bračko M, Pečnik T, Gadžijev EM, Serša G (2010) Towards treatment planning and treatment of deep-seated solid tumors by electrochemotherapy. Biomed Eng OnLine 9:10. doi:10.1186/1475-925X-9-10

Miklavčič D, Serša G, Brecelj E, Gehl J, Soden D, Bianchi G, Ruggieri P, Rossi CR, Campana LG, Jarm T (2012) Electrochemotherapy: technological advancements for efficient electroporation-based treatment of internal tumors. Med Biol Eng Comput 50:1213–1225. doi:10.1007/s11517-012-0991-8

Mir LM, Orlowski S, Poddevin B, Belehradek J (1992) Electrochemotherapy tumor treatment is improved by interleukin-2 stimulation of the host's defenses. Eur Cytokine Netw 3:331–334

Mir LM, Gehl J, Serša G, Collins CG, Garbay J-R, Billard V, Geertsen PF, Rudolf Z, O'Sullivan GC, Marty M (2006) Standard operating procedures of the electrochemotherapy: instructions for the use of bleomycin or cisplatin administered either systemically or locally and electric pulses delivered by the CliniporatorTM by means of invasive or non-invasive electrodes. Eur J Cancer Suppl 4:14–25

Neal RE 2nd, Garcia PA, Robertson JL, Davalos RV (2012) Experimental characterization and numerical modeling of tissue electrical conductivity during pulsed electric fields for irreversible electroporation treatment planning. IEEE Trans Biomed Eng 59:1076–1085

Neal RE 2nd, Rossmeisl JH, Robertson JL, Arena CB, Davis EM, Singh RN, Stallings J, Davalos RV (2013) Improved local and systemic anti-tumor efficacy for irreversible electroporation in immunocompetent versus immunodeficient mice. PLoS ONE 8:e64559. doi:10.1371/journal.pone.0064559

Neal RE 2nd, Millar JL, Kavnoudias H, Royce P, Rosenfeldt F, Pham A, Smith R, Davalos RV, Thomson KR (2014) In vivo characterization and numerical simulation of prostate properties for non-thermal irreversible electroporation ablation: characterized and Simulated Prostate IRE. Prostate. doi:10.1002/pros.22760

Neal RE 2nd, Garcia PA, Kavnoudias H, Rosenfeldt F, Mclean CA, Earl V, Bergman J, Davalos RV, Thomson KR (2015) In vivo irreversible electroporation kidney ablation: experimentally correlated numerical models. IEEE Trans Biomed Eng 62:561–569. doi:10.1109/TBME.2014.2360374

Neu WK, Neu JC (2009) Theory of Electroporation. In: Efimov IR, Kroll MW, Tchou PJ (eds) Cardiac Bioelectric Therapy. Springer, US, Boston, MA, pp 133–161

Pakhomova ON, Gregory BW, Pakhomov AG (2013) Facilitation of electroporative drug uptake and cell killing by electrosensitization. J Cell Mol Med 17:154–159

Peleg M (1995) A model of microbial survival after exposure to pulsed electric fields. J Sci Food Agric 67:93–99

Peleg M (2006) Advanced quantitative microbiology for foods and biosystems: models for predicting growth and inactivation. CRC series in contemporary food science. Taylor & Francis, Boca Raton

Pucihar G, Mir LM, Miklavčič D (2002) The effect of pulse repetition frequency on the uptake into electropermeabilized cells in vitro with possible applications in electrochemotherapy. Bioelectrochem Amst Neth 57:167–172

Pucihar G, Krmelj J, Reberšek M, Napotnik T, Miklavčič D (2011) Equivalent pulse parameters for electroporation. IEEE Trans Biomed Eng 58:3279–3288

Sack M, Sigler J, Frenzel S, Eing C, Arnold J, Michelberger T, Frey W, Attmann F, Stukenbrock L, Müller G (2010) Research on industrial-scale electroporation devices fostering the extraction of substances from biological tissue. Food Eng Rev 2:147–156. doi:10.1007/s12393-010-9017-1

Santillana Farakos SM, Frank JF, Schaffner DW (2013) Modeling the influence of temperature, water activity and water mobility on the persistence of Salmonella in low-moisture food. Int J Food Microbiol 166:280–293. doi:10.1016/j.ijfoodmicro.2013.07.007

Šel D, Lebar AM, Miklavčič D (2007) Feasibility of employing model-based optimization of pulse amplitude and electrode distance for effective tumor electropermeabilization. IEEE Trans Biomed Eng 54:773–781. doi:10.1109/TBME.2006.889196

Serša G, Miklavčič D, Čemažar M, Belehradek J, Jarm T, Mir LM (1997) Electrochemotherapy with CDDP on LPB sarcoma: comparison of the anti-tumor effectiveness in immunocompetent and immunodeficient mice. Bioelectrochem Bioenerg 43:270–283

Silve A, Guimerà Brunet A, Al-Sakere B, Ivorra A, Mir LM (2014) Comparison of the effects of the repetition rate between microsecond and nanosecond pulses: electropermeabilization-induced electro-desensitization? Biochim Biophys Acta BBA-Gen Subj 1840:2139–2151

Stone G, Chapman B, Lovell D (2009) Development of a log-quadratic model to describe microbial inactivation, illustrated by thermal inactivation of Clostridium botulinum. Appl Environ Microbiol 75:6998–7005. doi:10.1128/AEM.01067-09

Van Boekel M (2002) On the use of the Weibull model to describe thermal inactivation of microbial vegetative cells. Int J Food Microbiol 74:139–159. doi:10.1016/S0168-1605(01)00742-5

Weaver JC (1993) Electroporation: a general phenomenon for manipulating cells and tissues. J Cell Biochem 51:426–435

Weaver JC, Chizmadzhev YA (1996) Theory of electroporation: a review. Bioelectrochem Bioenerg 41:135–160. doi:10.1016/S0302-4598(96)05062-3

Yarmush ML, Golberg A, Serša G, Kotnik T, Miklavčič D (2014) Electroporation-based technologies for medicine: principles, applications, and challenges. Annu Rev Biomed Eng 16: 295–320. doi:10.1146/annurev-bioeng-071813-104622

Županič A, Miklavčič D (2011) Tissue heating during tumor ablation with irreversible electroporation. Elektrotehniški Vestn Engl Ed 78:42–47

Županič A, Kos B, Miklavčič D (2012) Treatment planning of electroporation-based medical interventions: electrochemotherapy, gene electrotransfer and irreversible electroporation. Phys Med Biol 57:5425–5440. doi:10.1088/0031-9155/57/17/5425